Comptes Rendus

Physique

Laurent Cormier, Laurence Galoisy, Gérald Lelong and Georges Calas

From nanoscale heterogeneities to nanolites: cation clustering in glasses

From everyday glass to disordered solids / *Du verre quotidien aux solides désordonnés*

From nanoscale heterogeneities to nanolites: cation clustering in glasses

Des hétérogénéités nanométriques aux nanolites : les agrégats cationiques dans les verres

Laurent Cormier[®] [*, a], **Laurence Galoisy**[®] [a], **Gérald Lelong**[®] [a] **and Georges Calas**[®] [a]

[a] Institut de Minéralogie, de Physique des Matériaux et de Cosmochimie (IMPMC) (Sorbonne Université, CNRS UMR 7590, Muséum national d'Histoire naturelle, IRD UMR 206), 4 place Jussieu, 75005 Paris, France

E-mails: laurent.cormier@sorbonne-universite.fr (L. Cormier), laurence.galoisy@upmc.fr (L. Galoisy), gerald.lelong@sorbonne-universite.fr (G. Lelong), georges.calas@upmc.fr (G. Calas)

Abstract. The structural behavior of cations in multicomponent oxide glasses cannot be described within a random network model, due to the presence of cation clusters that provide original properties. These clustering processes are even observed for cations that may occur at a percent level concentration, which makes it all the more spectacular. In particular, the structural and chemical characteristics of Zr^{4+}- and Fe^{2+}/Fe^{3+}-based clusters in (alumino)silicate glasses illustrate the link between the short-range order around cations and the formation of nanoscale heterogeneities. The structural characteristics of these Zr- or Fe-rich clusters are similar, as both are based on edge-sharing cation polyhedra. Cations may also occur in a network-forming position. In that case, cation sites are corner-linked with the silicate network. In such positioning, Pauling rules and local charge balance requirements will favor cations be diluted at a nanoscale. The topological constraints of these two types of local structure are stronger for the former than for the latter, as disorder effects are smaller for edge-sharing than for corner-sharing polyhedra. This may explain crystal nucleation during the growth of such ordered heterogeneities, giving rise to original properties that are illustrated in a large diversity of glassy materials encompassing high-tech glass-ceramics and volcanic glasses.

Résumé. Le comportement structural des cations dans les verres d'oxydes multicomposants ne peut pas être décrit dans un modèle de réseau aléatoire, en raison de la présence d'agrégats de cations à l'origine de propriétés originales. Ces processus de regroupement sont même observés pour les cations en faible concentration, ce qui le rend d'autant plus spectaculaire. En particulier, les caractéristiques structurales et chimiques des agrégats à base de Zr^{4+}- et de Fe^{2+}/Fe^{3+} dans des verres (alumino)silicates illustrent le lien entre l'ordre à courte portée autour des cations et la formation dhétérogénéités nanométriques. Les caractéristiques structurales de ces amas riches en Zr ou en Fe sont similaires, car les deux sont basées sur des polyèdres cationiques partageant des arêtes. Les cations peuvent également se trouver en position de formateur de réseau.

---

* Corresponding author.

Dans ce cas, les sites cationiques sont reliés au réseau silicaté. Dans un tel positionnement, les règles de Pauling et les exigences locales d'équilibrage des charges favoriseront la dilution des cations à l'échelle nanométrique. Les contraintes topologiques de ces deux types de structure locale sont plus fortes pour le premier que pour le second, car les effets de désordre sont plus faibles pour le partage des polyèdres par arêtes que pour le partage par sommets. Cela peut expliquer la nucléation du cristal pendant la croissance de ces hétérogénéités ordonnées, donnant lieu à des propriétés originales qui sont illustrées dans une grande diversité de matériaux vitreux englobant les vitrocéramiques de haute technologie et les verres volcaniques.

1. Introduction

A glass is defined by a lack of periodicity and long-range order and a specific thermodynamic behavior with the existence of the glass transition. Information about the structure of oxide glasses and melts at a molecular-scale helps rationalize and understand their properties [1, 2]. In multicomponent glasses, network-forming cations occur in tetrahedral sites or similar network position, the network-forming role arising from well-defined topological relationships within the polymeric network. Cations occur either as modifiers, playing a depolymerizing role of the polymeric framework, or as charge compensators, in the vicinity of charge-defective sites in the glassy network. These structural properties govern most glass properties. However, cation clustering is not predicted in such a simplified model of glass structure, despite increasing evidence of its importance.

Glass structure remains a challenge, because glasses possess no long-range structural periodicity or symmetry. Information about short- and medium-range organization around most cations is limited, due to the non-directional and partly ionic nature of the bonds between cations and oxygen atoms. The use of specific structural techniques and modeling codes has demonstrated that the structure of glasses does not obey a random distribution and cannot be described as a homogeneous atomic distribution [2]. In the modified random network (MRN) model proposed by Greaves [3], the structure of multicomponent glasses is no more described as being homogeneously random (continuous random network model [4]) in contrast to silica and other network glasses. This model proposes that non-framework cations (alkalis and alkaline-earths, transition elements...) are not distributed at random throughout the silicate framework. These cations rather occur within domains percolating through the polymerized network constituted by SiO_4 tetrahedra and forming less polymerized and more ionic regions. The polyhedral units characterize the short-range order (SRO). The structure beyond the first shell of nearest neighbors corresponds to the medium range order (MRO), usually observed up to 1–2 nm [5], which obeys the basic crystal chemical principles (e.g., Pauling rules). Such a model has been successful to rationalize spectroscopic, structural and macroscopic properties of glasses [6, 7].

Direct evidence of cation clustering and structural heterogeneity of glasses was provided by neutron diffraction experiments with isotopic substitution. This original approach has demonstrated the existence of Ca–Ca, Ni–Ni and Ti–Ti pairs in Ca-, Ni- and Ti-bearing glasses, respectively [8]. The geometry of these atomic pairs is based on edge-sharing sites, corresponding to 5-coordination for Ni^{2+} and Ti^{4+} or 6-coordination for Ca^{2+}. In addition, a spectacular cation clustering, at least up to 0.6 nm diameter, has been observed by X-ray absorption spectroscopy (XAS) in low-alkali borate glasses containing minor M^{2+} cations (M = Ni, Co, Zn) [9].

The importance of these structural heterogeneities appears in the glass transition phenomenon itself. In fact, dynamical heterogeneities are considered as an important concept with regions of slow and high mobility, the importance of which increases as the glass transition temperature (T_g) is approached by the system. These domains are associated with chemical or structural

fluctuations. In Molecular Dynamics simulations of CaO–Al$_2$O$_3$–SiO$_2$ glasses, dynamical heterogeneities have been identified with compositional and structural fluctuations associated with regions enriched with CaO and Al$_2$O$_3$ (high mobility) or SiO$_2$ (low mobility) [10]. Over the last 10 years, the importance of nanoscale heterogeneities has been increasingly recognized due to the emergence of new techniques, notably by directly imaging the spatial and chemical fluctuations using Transmission Electron Microscopy (TEM) [11–13]. These techniques allow a visualization of the nanoscale glass structure, especially as extended phase separation occurs [14].

A deeper knowledge of the MRO is critical for an understanding of a wide range of macroscopic properties, including mechanical and optical properties or crystallization processes [12, 15–17]. For instance, the clustering of rare earth ions in silica glass degrades the performance of optical devices, as it favors non-radiative energy transfers causing in turn a quench of fluorescence. Addition of a codopant, such as Al, improves the spatial distribution of rare earth ions R, forming R–O–Al bonds (with rare-earth compensating the charge deficit of AlO$_4$ tetrahedra) at the expense of R–O–R linkages, leading to the disappearance of these rare-earth clusters [2].

In this paper, we analyze recent results that have been obtained on cluster-containing glasses trough a multi-technique approach, using diffraction and spectroscopic techniques complemented by numerical modeling. These data show that the structural behavior of cations cannot be predicted by considering a random network model of multicomponent oxide glasses. The structural heterogeneities are observed for the case of Zr (part 2) and the influence of this organization on the crystallization properties is considered (part 3). We then focus the discussion on the case of Fe, showing experimental proofs of Fe segregation even at dilute Fe concentration (part 4) and in natural glasses (part 5). In these latter materials, Fe heterogeneities are likely related to the presence of nanolites that strongly impact viscosity properties. In part 6, we discuss how both Zr- and Fe-clusters are based on edge-sharing cation polyhedra in which cations are segregated. By contrast, cations in a network-forming or network-modifying position show only corner-sharing linkages with the (alumino)silicate network. The topological constraints of these two types of local structure are stronger for the former than for the latter. Indeed, degrees of freedom and hence disorder effects are smaller for edge-sharing than for corner-sharing polyhedra. The structural and chemical characteristics of Zr- and Fe-clusters help rationalize the role of these elements on the properties of glasses and glass-ceramics, including volcanic glasses and high-tech glasses. These structure-property relationships are observed even in diluted glasses, which makes these clustering processes all the more spectacular.

2. Heterogeneities in glasses: a typical case with Zr^{4+}

Because chemical selectivity is needed when investigating multicomponent glasses, XAS, associating Extended X-ray Absorption Fine Structure (EXAFS) and X-ray Absorption Near Edge Structure (XANES) spectroscopies, has been extensively used, giving detailed information on MRO [18]. Among transition elements, Zr^{4+} is particularly attractive due to its stability in a large diversity of coordinated sites. In silicate glasses, Zr^{4+} is known to play a stabilizing or nucleating role, depending on the coexisting cations [19–21]. We have investigated the Zr^{4+} environment in different aluminosilicate glasses with monovalent and divalent cations using XAS [22]. A combination of K- and L-edge XANES spectra unambiguously revealed that the Zr^{4+} environment differs between glasses containing alkalis (Li and Na aluminosilicate glasses) or divalent cations (Mg, Ca, Zn). Zirconium coordination does not appear to influence its nucleating role (Figure 1). Indeed, in alkali aluminosilicate glasses, Zr^{4+} dramatically favors the nucleation rate in Li-bearing glasses and, by contrast, does not enhance crystallization in Na-bearing glasses. Therefore, Zr coordination is not the only relevant parameter to determine the ability for Zr^{4+} to act as a nucleating agent. By and large, for the main nucleating agents in glasses (i.e. Zr^{4+} or
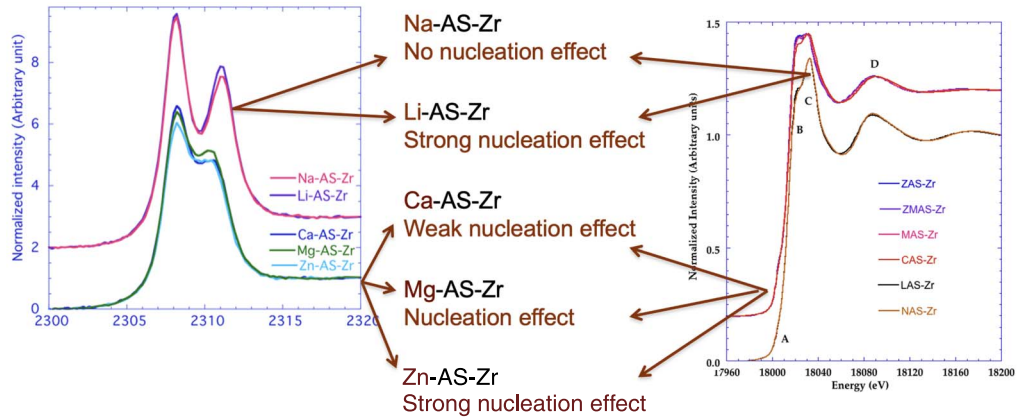
Figure 1. XANES spectra at L_2-edge (left) and K-edge (right) for zirconium in various aluminosilicate glasses showing more or less high degree of nucleation, as determined by Differential Scanning Calorimetry (adapted from [22]). Two groups of spectra can be distinguished: spectra for monovalent cations (Na^+ and Li^+) and divalent cations (Ca^{2+}, Mg^{2+}, Zn^{2+}) corresponding to different Zr environments.
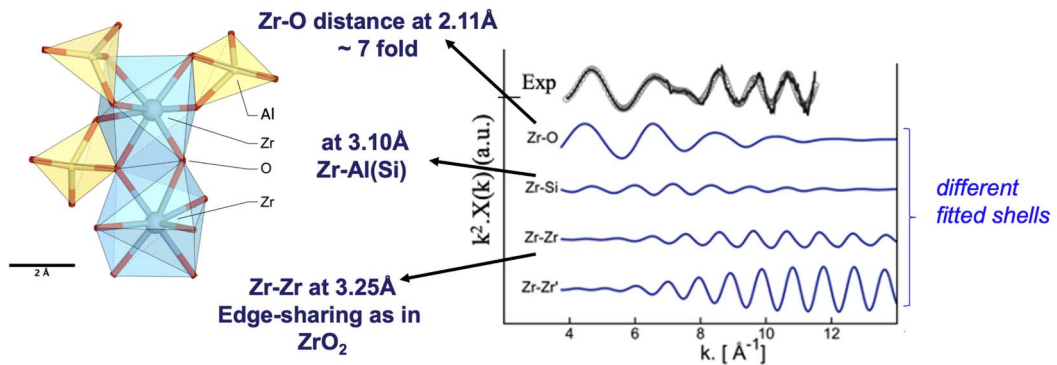

Figure 2. EXAFS spectra at Zr K-edge in a Mg-aluminosilicate glass and is decomposition in different shells of neighbors allowing proposing a structural model for Zr environment (adapted from [20]).

Ti^{4+}), there is no evidence that specific sites or coordination numbers can be proposed to favor nucleation [23]. The key factor governing nucleation/crystallization lies instead in the medium range organization.

Interestingly, XAS is able to probe MRO (Figure 2). For instance, EXAFS data on Mg aluminosilicate glasses (MgAS) containing 4 mol% ZrO_2 show the contribution of the next-nearest neighbors (Si and Zr) and provide constraints to model Zr environment. This approach demonstrates the presence of strong, edge-sharing linkages between 7-coordinated Zr sites, a local structure that mimics that encountered in m-ZrO_2. Conversely, in most Zr-bearing alkali glasses, Zr is 6-coordinated and is only corner-linked to Si/Al-sites (and charge-compensating cations).

The close proximity between Zr atoms inferred from EXAFS in the initial MgAS glass can be directly visualized using HAADF-STEM (High Angle Annular Dark Field—Scanning Transmission Electron Microscope) imaging (Figure 3). Due to the chemical contrast of the HAADF technique, it is possible to ascribe the bright regions to a greater local concentration of Zr atoms having
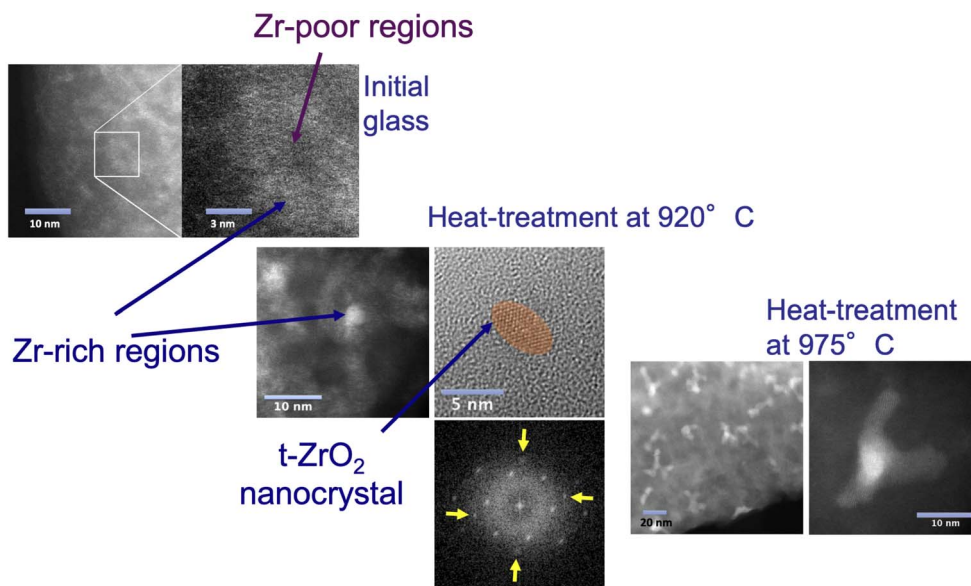
Figure 3. HAADF-STEM images of Mg-aluminosilicate glass containing 4 mol% ZrO_2. The bright regions correspond to Zr-rich regions. With heat treatment and nucleation, these regions become brighter and are the preferential location for ZrO_2 crystallization (adapted from [25]).

a diffuse interface with the remaining glass (dark regions in Figure 3). The amorphous Zr-rich heterogeneities have a size larger than the diameter of critical nuclei, usually observed with a size of 2–5 nm [20–24]. Therefore, these structural fluctuations cannot be considered as precritical nuclei but as intrinsic components of the structural organization of the glass matrix. Figure 3 corresponds to a typical MRN topology: the cations such as Zr form channels within the depolymerized network structure, resulting in a nanosegregation of network-forming (silicate groups) and modifying components (Zr and Mg).

The formation of nanoscale heterogeneities is confirmed by Small Angle Neutron Scattering data (SANS) (Figure 4), obtained at the Center for Neutron Research (NIST, USA). In fact, the Zr-free MgAS glass already exhibits small fluctuations in the SANS signal, though these fluctuations cannot be observed in HAADF-STEM imaging due to the lack of chemical contrast between the components of this glass. This reflects inherent fluctuations within the structure of aluminosilicate glasses. Tentatively, these fluctuations can be associated to a non-random distribution of Al species around Si. As the MgAS glass contains important fraction of five- and six-fold coordinated Al ([5]Al and [6]Al, respectively) [26], we can speculate that AlO_5 and AlO_6 polyhedra have important edge-sharing linkages, resulting in denser regions formed by [5]Al–[6]Al-rich domains. As a support to this hypothesis, a heterogeneous distribution of Al has been observed in a phase-separated Al_2O_3–SiO_2 glass, where the fraction of highly coordinated Al species are more abundant in regions having a large Al_2O_3 content [27].

As a consequence of the introduction of ZrO_2, the size of inhomogeneities detected by SANS increases. Addition of ZrO_2 impacts the mesoscopic organization of the glass structure. The presence of Zr-rich regions can be explained by Zr^{4+} sites being either in 6- or 7-fold coordination and competing less favorably than Al^{3+} cations for charge-balancing cations [28, 29]. They tend to segregate by edge-sharing linkages. Edge-sharing of Zr^{4+} sites is consistent with the short
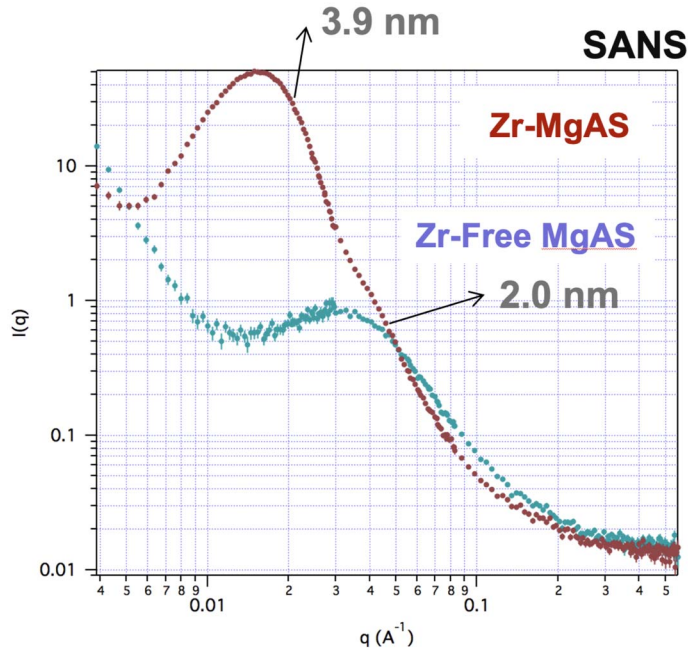
Figure 4. SANS data for a Mg-aluminosilicate glass without and with Zr, showing a feature characteristic of fluctuations with size of 2 to 3.9 nm.

Zr–Zr distances (~3.1 Å) extracted from EXAFS data (Figure 2) and characteristic of edge-sharing linkages [20]. EXAFS cannot distinguish the nature of the other next-nearest neighbors since Mg, Al and Si have close X-ray scattering amplitudes. However, ZrO_7 polyhedra are more likely edge-shared with AlO_5 or AlO_6 units than with a tetrahedral unit because the latter case yields to strong distortion to accommodate polyhedra with large different sizes. Pauling rules also favor the presence of high-coordinated sites to avoid the overbonding of the O ligands.

These amorphous nanoscale chemical heterogeneities appear unavoidable and inherent to the glass structure. Even a fast-quenched glass, showing no sign of macroscopic phase separation such as opalescence, exhibits Zr segregation [11]. However, at a slow quench rate, a clear glass-in-glass immiscibility associated with a macroscopic opalescence, can be identified. This result suggests that heterogeneities as those displayed in Figure 3 are likely the first step in the phase separation process occurring above T_g. An unknown and crucial issue would be to determine whether such heterogeneities appear during cooling in the supercooled liquid state, near T_g, or if they are already present at high temperatures in the molten state. A recent study on the solubility of Zr in peraluminous glasses has concluded that segregation is related to the presence of a sub-liquidus immiscibility field in MgAS glasses, as heterogeneities increase in size at high Al/Si ratios [30]. This study also emphasizes the role of Al^{3+} cations and the preferential association of Zr and Al in the same demixed regions.

Since the pioneering work of Dargaud and co-workers [11, 25], further HAADF-STEM investigations have confirmed the presence of heterogeneities in several glass systems, often close to an amorphous-amorphous separation: Ta-bearing Li aluminosilicate glasses [31], Ca aluminosilicate [16], basaltic [32] or metallic glasses [17, 33]. Though this technique requires a good chemical contrast between glass constituents, it has been recently demonstrated that it is possible to distinguish Al-rich and Si-rich regions in a phase separated Al_2O_3–SiO_2 glass [27, 34].

3. From heterogeneities to nucleation

These static structural fluctuations play a crucial role in the crystallization process, as they are often the first step evoked during crystalline nucleation [14, 35–38]. During heat treatment, Zr-rich regions tend to merge: the bright regions in Figure 3 become brighter with sharper boundaries than in the starting glass after a heating treatment at 920 °C. We observe that nucleation forms, at first, tetragonal ZrO_2 nanocrystals preferentially at the diffuse connections between the Zr-rich domains, showing the direct relationships between inhomogeneities and nucleation pathways [25]. The static fluctuations induce variations in the local barriers to nucleation for the different regions of the system, which can facilitate the formation of the primary nanocrystals [39]. The segregation of Zr^{4+} ions acts as an activated mechanism favoring the local reorganization of the structure towards a crystalline order. At further heating treatment of 975 °C, these ZrO_2 nanoparticules only slightly grow in size. The glassy matrix surrounding the crystals shows weak contrast fluctuations suggesting that Zr^{4+} ions are almost completely incorporated within the crystalline regions.

In SiO_2–Al_2O_3–MgO–ZrO_2 glasses, the nucleation of ZrO_2 occurs prior to the formation of β-quartz solid-solution [20, 35, 38]. This first step is also associated with an increase of the SAXS signal indicating critical nuclei sizes of ~2 nm [40]. During this initial step, [5]Al and [6]Al may diffuse within crystalline ZrO_2, since doping of ZrO_2 is often encountered, particularly by trivalent elements [41]. We have characterized by ^{27}Al NMR the Al environment in a glass heat treated at the temperature of ZrO_2 nucleation (spectrum not shown). No increase in the proportion of AlO_6 units and no narrow peak characteristic of crystalline phases, are detectable. This result rules out the possibility of significant doping of Al^{3+} in initial nano-zirconia. An alternative explanation is that Al^{3+} ions are expelled at the boundary of the ZrO_2 nano-crystals. This behavior was indeed observed in an aluminosilicate glass containing TiO_2 and ZrO_2, in which the first crystallizing phase is $ZrTiO_4$ [24]. An Al rich layer was detected by electron energy-loss spectroscopy and a specific interaction was proposed between $ZrTiO_4$ and Al^{3+}, in good agreement with the present results. This scenario has attractive advantages. It provides a diffusion barrier preventing particle growth and Ostwald ripening. Furthermore, the remaining glass corresponding to Si-rich regions associated with AlO_4 units can favor the formation of β-quartz.

The experimental evidence of heterogeneities supports recent simulation studies showing critical density fluctuations at the origin of nucleation in various systems such as colloidal particles or protein solutions [42, 43]. The subtle exploration of MRO contradicts a fundamental hypothesis of the Classical Nucleation Theory that assumes an initial homogeneous state. This represents a key step to resolve the theory/experiment mismatch observed in the rate of nucleation kinetics.

The nanoscale organization of glasses can be a major route, yet poorly explored, to finally design the glass structural organization. Manipulating the extent of heterogeneities could be exploited as an effective strategy to master the nanostructure and crystal formation in glass-ceramics [31, 44].

4. Fe clusters in silicate glasses

Cation clustering in concentrated glasses may be put in evidence by comparing the experimental MRO with the one expected from glass stoichiometry. Combining neutron diffraction with Fe isotope substitution and Empirical Potential Structure Refinement (EPSR) simulations [45], the existence of three Fe-populations in a $NaFeSi_2O_6$ glass was evidenced, by contrast to the structure of the corresponding crystalline phase, which contains only octahedral Fe^{3+}. Majority network-forming [4]Fe^{3+} (about 59% of total Fe) shares corners with SiO_4 tetrahedra, and is randomly
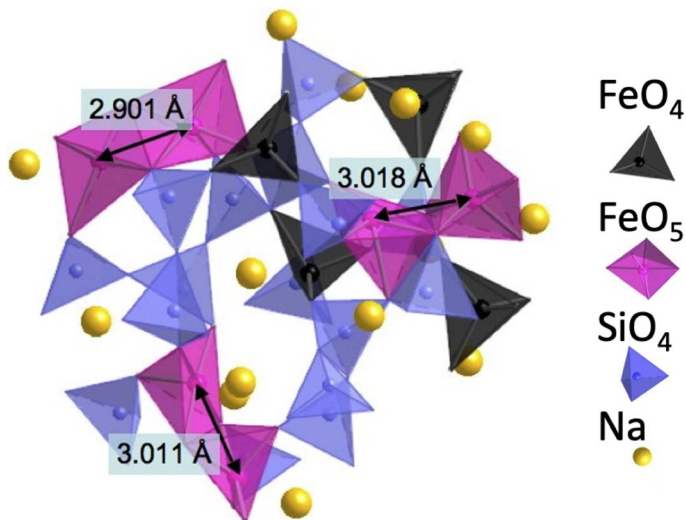
Figure 5. Medium range organization of $NaFeSi_2O_6$, as derived from EPSR simulations. It shows a clustering of Fe^{3+}, due to the high fraction of 5-coordinated Fe^{3+} sites. This structure is different from that of the $NaAlSi_2O_6$ glass, based on a random distribution of tetrahedral Al^{+3} sites [45].

distributed in agreement with a network-forming role, similar to that of [4]Al^{3+} in $NaAlSi_2O_6$ glass (Figure 5). By contrast, minority [5]Fe^{2+} and [5]Fe^{3+} cations (about 36% of total Fe) tend to segregate. This provides an original picture of the structure of this glass, differing from the tridimensional structure expected from its stoichiometry and observed in $NaAlSi_2O_6$ glass [46]. By contrast to most Fe-bearing sodium silicate glasses, $NaFeSi_2O_6$ glass crystallizes into an isochemical crystalline polymorph [47]. The presence of segregated high-coordinated Fe-sites may explain the ability for this glass to crystallize in a pyroxene structure.

Clustering efficiency may be quantified by the relative proportion of Fe in the second coordination shell around Fe. This parameter is only dependent on glass stoichiometry if cations are randomly distributed. For $NaFeSi_2O_6$ glass, EPSR simulations indicate a value of 0.42, larger than the value of 0.33 predicted in a random distribution model. This anomalous behavior of Fe cations arises from an efficient clustering of [5]Fe sites. A similar contrast between randomly distributed [4]Fe and clustered [5]Fe sites has been evidenced by molecular dynamics simulations in $Li(Al,Fe)Si_2O_6$ glasses [48].

Edge-sharing linkages between Fe^{2+} and Fe^{3+} sites in Fe clusters give rise to unusual optical and magnetic properties. A noticeable consequence of the presence of Fe^{2+} and Fe^{3+} in silicate glasses is their color. At low Fe concentration, oxide glasses melted in air exhibit light greenish coloration due to the presence of minority Fe^{2+}, as Fe^{3+} *d–d* crystal field transitions are spin forbidden and do not contribute to glass color. At high Fe-concentration, glasses exhibit a dark brown color caused by a Fe^{2+}–Fe^{3+} intervalence charge transfer (IVCT), which causes electron-hopping processes between edge-sharing [5]Fe^{2+} and [5]Fe^{3+} sites [49, 50]. As electron hopping is easier if the two sites have similar symmetries [50], an efficient coloration is consistent with Fe-clusters based on edge-sharing [5]Fe^{3+} and [5]Fe^{2+}.

Electron Paramagnetic Resonance (EPR) provides unique information on the structure of glasses containing paramagnetic ions and associated superparamagnetic clusters [51]. The presence of Fe-clusters in glasses has been observed at Fe-concentration as low as 0.1 mol% Fe_2O_3 using EPR [52,53]. The nature of these clusters has been investigated recently by Fe K-edge
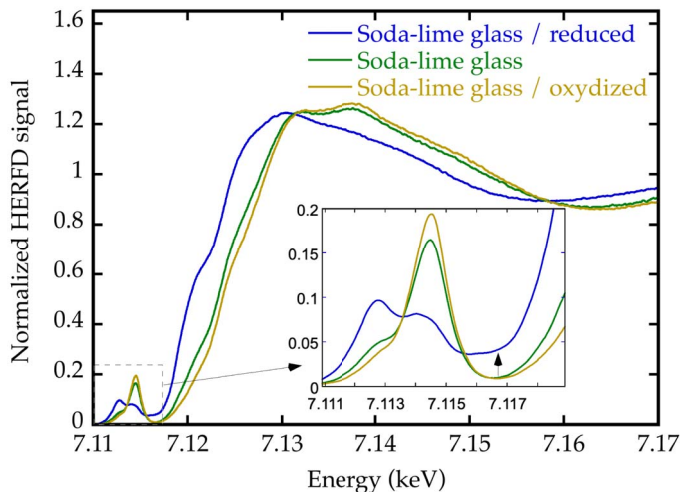
Figure 6. Effect of oxidation conditions on HERFD-XAS spectra at the Fe K-edge in soda lime silicate glasses containing 0.5 wt% of Fe_2O_3 and synthesized under reducing (blue) or oxidizing conditions (yellow) and in air (green).

HERFD-XANES (High Energy Resolution Fluorescence Detected-XANES) for soda-lime silicate glasses synthesized under different oxidation conditions (Figure 6). The reduced glass presents an additional absorption at an intermediate energy between the pre-edge and the main edge, around 7116 eV. This feature is not visible in the case of glasses synthesized under air or under oxidizing conditions for which there is almost no absorption between the pre-edge and the main edge. Similar features have been previously observed in hematite, ferrihydrite [54] or in maghemite and Fe_3PO_7 [55]. They are ascribed to delocalized states due to interactions caused by the presence of Fe ions as a second neighbor, via an oxygen-mediated $4p$-$3d$ intersite hybridization $(Fe(4p)–O(2p)–Fe'(3d))$ [56]. These covalency effects indicate edge-linkages between Fe-polyhedra and involve $^{[6]}Fe^{3+}$ or $^{[5]}Fe^{3+}$ cations preferably to $^{[4]}Fe^{3+}$, as observed in minerals [57]. By analogy, iron clusters in glasses would be favored by Fe^{3+} located in [5]-fold or [6]-fold coordinated sites: this could suggest that reduced glasses contain a higher proportion of Fe^{3+} occurring in 5- and/or 6-fold coordination than the corresponding oxidized glasses that rather favor non-connected tetrahedral Fe^{3+} sites. This is a consequence of the Lowenstein exclusion rule [58], which predicts that the linkage between tetrahedral sites of trivalent cations is energetically unfavored as it leads to the formation of oxygen triclusters.

There is a clear trend for a heterogeneous Fe distribution in glasses. Among the various Fe species, $^{[4]}Fe$ is randomly distributed in the network and shares corners with other cationic (framework) tetrahedra. The FeO_5 polyhedra tend to share edges among themselves. This trend towards $^{[5]}Fe$ clustering confirms the presence of domains enriched in network modifier cations, as predicted by the modified random network model.

5. Fe clusters in natural obsidians

Obsidians are volcanic glasses that are widespread and possess most glass properties: glass transition, density, brittleness, hardness... They usually contain about 1 wt% Fe, but most common colors of obsidians, ranging from brownish to smoke-grey to black, with infrequent mahogany
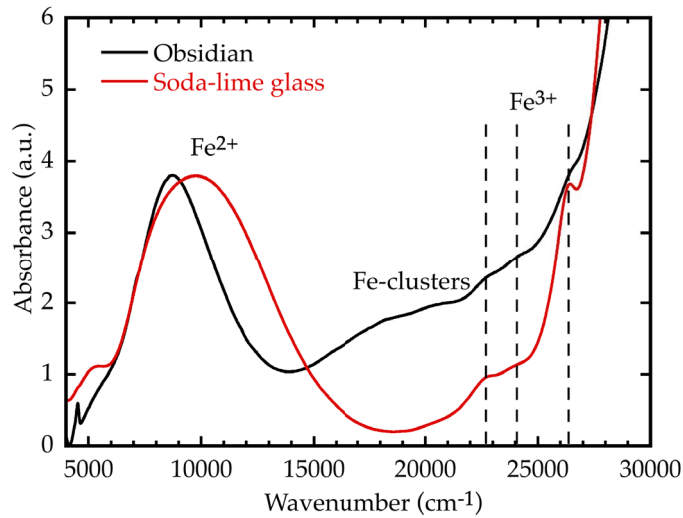
Figure 7. Comparison of the optical absorption spectra of a Lipari obsidian (black) and a soda-lime glass (red). The spectra are normalized to the intensity of the Fe^{2+} absorption band near 10,000 cm^{-1}. Vertical dashed lines indicate that the weak Fe^{3+} transitions in the UV and near-UV occur at the same position. By contrast, the position and width of the Fe^{2+} absorption band near 10,000 cm^{-1} are different in obsidian and synthetic soda-lime glass, showing a different Fe-speciation.

or green hues [59], differ from the greenish synthetic silicate glasses. As resulting from melt degassing during ascent and cooling during emplacement, their peculiar formation conditions have attracted interest since decades to understand the origin of their original properties.

Iron speciation in obsidians reveals the presence of Fe-clusters as shown by various spectroscopic methods, such as EPR or Mössbauer [51, 60, 61] or Raman micro-spectroscopy [62]. Rock magnetism confirms the presence of diluted Fe^{3+} in the glassy matrix and of magnetite nanolites [63]. Nanolites were recently suggested to play a significant role in volcanic processes, during the transition from effusive to explosive regime [64]. Spectroscopic data have shed light on the correlation between Fe-speciation and the optical properties of obsidians demonstrating that the majority of Fe-sites does not occur within the glass structure but belong to mixed-valence, magnetite-like clusters [65]. These clusters are responsible for the dark coloration of obsidians through electron hopping between neighboring Fe^{2+} and Fe^{3+} sites. At a molecular scale, these clusters are unique witnesses of the extensive degassing of a rising silicic magma.

The optical absorption spectrum of an obsidian glass is quite different from that of a synthetic Fe-bearing glass (Figure 7). Located near 10,000 cm^{-1}, the Fe^{2+} crystal-field absorption band is Gaussian-shaped and significantly narrower than in the spectrum of a synthetic silicate glass. It indicates an octahedral coordination with a limited site distribution between regular and slightly distorted sites. The optical properties of magnetite-like clusters give rise to such a band [66]. The high intensity of this band is explained by an exchange-coupled pairing process enhanced by a coupling between neighboring Fe^{2+}-sites contained in the Fe-clusters [67]. This is a marked difference with synthetic glasses where the Fe^{2+} band shows an asymmetrical shape in relation with a broad site distribution between $^{[5]}Fe^{2+}$ and $^{[4]}Fe^{2+}$ sites. Crystal-field bands for Fe^{3+} are located at the same positions in obsidian and synthetic glasses, but with a lower intensity in the former than in the latter, due to different Fe-redox values.
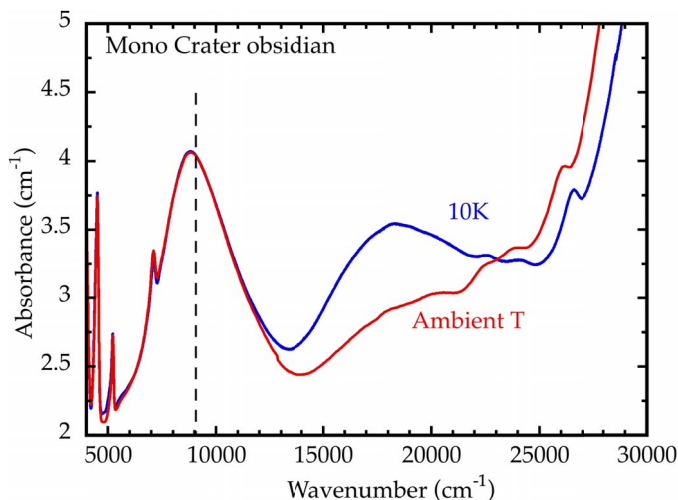
Figure 8. Optical absorption spectra of Mono Crater (Panum Dome #2) obsidian, at ambient T and 10 K. The broad band near 18,000 cm^{-1} is sharply intensified at 10 K, an indication of an intervalence charge transfer Fe^{2+} ⇔ Fe^{3+}, caused by the presence of Fe-rich clusters in obsidian. The UV cutoff (that corresponds to an oxygen to metal charge transfer) shifts to higher wavenumbers. By contrast, the Fe^{2+} absorption band located near 10,000 cm^{-1} remains unchanged.

The transmission window, in the visible region, is obscured by a broad absorption band that contributes to the black color of most obsidians (Figure 7). At low temperature, the intensity of this band increases dramatically (Figure 8), a signature specific of a Fe^{2+} ⇔ Fe^{3+} IVCT. Indeed, IVCT intensity increases with decreasing temperature, as observed in a large number of minerals [68]. This property has been explained by an exchange-coupling model [69]. By contrast, the Fe^{2+}crystal-field band in synthetic nanomagnetites, at the same position as the one found in obsidians, retains a temperature independence of the wavenumber and intensity values [66]. The presence of an IVCT is a direct consequence of Fe-clustering in obsidians. The shape of the IVCT band shows a possible additional contribution from a Fe^{2+} ⇔ Ti^{4+} charge transfer. The presence of Ti-magnetite-like clusters in obsidians may be at the origin of Ti-rich magnetite nuclei.

At room temperature, the EPR spectra of obsidians are characterized by a broad and intense signal linked to superparamagnetic clusters encompassing the whole field range, above which are superimposed weak narrow signals (1500 G and 3500 G) of paramagnetic (isolated) Fe^{3+} (Figure 9). The EPR data obtained at low temperature (down to 77 K) are different. The intensity of the superparamagnetic contribution decreases sharply, indicating the presence of superparamagnetic clusters (Figure 9). These spectacular variations arise from magnetic coupling involving Fe^{3+} ions within the clusters. By contrast, the intensity of the paramagnetic isolated Fe^{3+} signals increases with decreasing temperature, following a Curie's law in 1/T that characterizes their paramagnetic behavior [65]. These data confirm the pioneering studies of Regnard *et al.* [61], based on low temperature Mössbauer spectra recorded in presence of an external magnetic field, which gave the first evidence of ultra-fine magnetite-like clusters in obsidians.

6. Discussion and conclusion

Information about the molecular-scale structure of multicomponent glasses comes from a combination of spectroscopic and diffraction/scattering measurements complemented by numerical
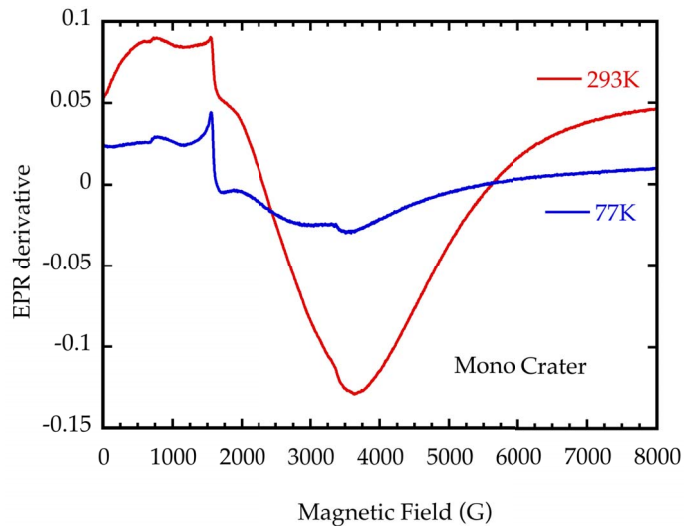
Figure 9. X-band Electron Parmagnetic Resonance signal of Fe^{3+} at 293 K (red) and at 77 K (black). The sharp signal near 1500 G and the weak features near 700 G and 3200 G are typical signatures of (paramagnetic) diluted Fe^{3+}. The broad contribution in the obsidian spectrum at room temperature is attenuated at 77 K, indicating the presence of Fe^{3+} in superparamagnetic Fe-rich clusters.

modeling, providing information on local geometry, site symmetry, and the nature of the chemical bonds. These data have resulted in an improved knowledge of the structural properties of glass components in oxide glasses, demonstrating a contrasted behavior between the polymeric network and the cations. By contrast to the largely covalent, directional bonds between network formers and oxygen that are associated to low values of diffusion coefficients, the ionic character of the cation-oxygen bonds facilitates their diffusion within the glass structure. In simulated silicate melts, the diffusion coefficients of Ca and Na may be larger than that of Si by 3 and 5 orders of magnitude, respectively, at 2000 K [70]. This distinct nature of the chemical bonds between network formers and cations favors a heterogeneous cation distribution and may lead to the formation of clusters and crystallization nuclei.

The structure of silicate glasses is based on a short-range order, which obeys the basic rules of crystal-chemistry [71, 72]. A random network model, proposed by Warren as an extension of the Zachariasen's model [73], gives only a partial view on the behavior of cations in glasses. It assumes that most cations are randomly distributed, filling the interstices of the polymerized network. This oversimplified representation of glass structure, in which cations are not expected to occur in well-defined sites, has been experimentally dismissed, resulting in the more recent modified random network (MRN) model [3, 6]. MRN recognizes an intrinsic heterogeneous nature of glass structure. It incorporates the covalent bonding of silicate tetrahedra with the ionic nature of the cation-oxygen bonds in a heterogeneous picture of the silicate glass structure. It recognizes cation–cation interactions, providing a rationale for a large range of glass properties, such as cation diffusion, glass dissolution, optical properties, etc. . . .

The chemical or structural fluctuations in glasses here presented demonstrate some similarities between two different cations, Zr^{4+} and $Fe^{2+/3+}$, shedding light on the mechanisms of amorphous to crystal transformation. Provided a local charge compensation exists, tetrahedral Fe^{3+} and octahedral Zr^{4+} correspond to a network-forming position with cation polyhedra being corner shared with the glassy network, as indicated by the Fe–Si and Zr–Si contributions evidenced in

the EXAFS spectra. In that case, the MRO is not compatible with the formation of cation clusters. By contrast, Fe- and Zr-rich clusters are based on edge sharing cation polyhedra, in a topological configuration not predicted by a random model. Edge sharing linkages provides more topological constraints than corner sharing, following the basic rules of structural chemistry [74]. As a consequence, an edge sharing geometry shows a more limited structural disorder as compared with a corner sharing geometry, which may also induce a local ordering favoring crystal nucleation. Such edge-sharing topology favors also cation–cation interactions and results in original glass properties, e.g. color or magnetic properties.

Conflicts of interest

Authors have no conflict of interest to declare.

Acknowledgements

References

[1] G. Calas, L. Cormier, L. Galoisy, P. Jollivet, "Structure-property relationships in multicomponent oxide glasses", *C. R. Chim.* **5** (2002), p. 831-843.

[2] G. N. Greaves, S. Sen, "Inorganic glasses, glass-forming liquids and amorphizing solids", *Adv. Phys.* **56** (2007), p. 1-166.

[3] G. N. Greaves, "EXAFS and the structure of glass", *J. Non-Cryst. Solids* **71** (1985), p. 203-217.

[4] W. H. Zachariasen, "The atomic arrangement in glass", *J. Am. Ceram. Soc.* **54** (1932), p. 3841-3851.

[5] S. R. Elliott, "Medium-range structural order in covalent amorphous solids", *Nature* **354** (1991), p. 445-452.

[6] G. N. Greaves, "EXAFS for studying corrosion of glass surfaces", *J. Non-Cryst. Solids* **120** (1990), p. 108-116.

[7] G. N. Greaves, K. L. Ngai, "Reconciling ionic-transport properties with atomic structure in oxide glasses", *Phys. Rev. B* **52** (1995), p. 6358-6380.

[8] L. Cormier, L. Galoisy, J.-M. Delaye, D. Ghaleb, G. Calas, "Short- and medium-range structural order around cations in glasses: a multidisciplinary approach", *C. R. Acad. Sci. Sér. IV* **2** (2001), p. 249-262.

[9] L. Galoisy, L. Cormier, G. Calas, V. Briois, "Environment of Ni, Co and Zn in low alkali borate glasses: information from EXAFS and XANES spectra", *J. Non-Cryst. Solids* **293–295** (2001), p. 105-111.

[10] K. D. Vargheese, A. Tandia, J. C. Mauro, "Origin of dynamical heterogeneities in calcium aluminosilicate liquids", *J. Chem. Phys.* **132** (2010), article no. 194501.

[11] O. Dargaud, L. Cormier, N. Menguy, G. Patriarche, "Multi-scale structuration of glasses: Observations of phase separation and nanoscale heterogeneities in glasses by Z-contrast scanning electron transmission microscopy", *J. Non-Cryst. Solids* **358** (2012), p. 1257-1262.

[12] K. A. Kirchner, D. R. Cassar, E. D. Zanotto, M. Ono, S. H. Kim, K. Doss, M. L. Bødker, M. M. Smedskjaer, S. Kohara, L. Tang, M. Bauchy, C. J. Wilkinson, Y. Yang, R. S. Welch, M. Mancini, J. C. Mauro, "Beyond the average: spatial and temporal fluctuations in oxide glass-forming systems", *Chem. Rev.* **123** (2023), no. 4, p. 1774-1840.

[13] T. Komatsu, T. Honma, "Nanoscale composition fluctuations and crystallization process: case study in Li_2O–SiO_2 based glasses", *Int. J. Appl. Glass Sci.* **13** (2022), no. 4, p. 591-609.

[14] W. Vogel, "Phase separation in glass", *J. Non-Cryst. Solids* **25** (1977), p. 170-214.

[15] W. Feng, D. Bonamy, F. Célarié, P. C. M. Fossati, S. Gossé, P. Houizot, C. L. Rountree, "Stress corrosion cracking in amorphous phase separated oxide glasses: a holistic review of their structures, physical, mechanical and fracture properties", *Corros. Mater. Degrad.* **2** (2021), p. 412-446.

[16] K. Nakazawa, T. Miyata, S. Amma, T. Mizoguchi, "Identification of nanometer-scale compositional fluctuations in silicate glass using electron microscopy and spectroscopy", *Scr. Mater.* **154** (2018), p. 197-201.

[17] F. Zhu, S. Song, K. M. Reddy, A. Hirata, M. Chen, "Spatial heterogeneity as the structure feature for structure–property relationship of metallic glasses", *Nat. Commun.* **9** (2018), article no. 3965.

[18] L. Galoisy, "X-ray absorption spectroscopy in geosciences: Information from the EXAFS region", in *Spectroscopic Methods in Mineralogy* (G. Papp, T. G. Weiszburg, A. Beran, E. Libowitzky, eds.), Mineralogical Society of Great Britain and Ireland, Germany, 2004, p. 553-587.

[19] G. Calas, L. Galoisy, L. Cormier, G. Ferlat, G. Lelong, "The structural properties of cations in nuclear glasses", *Procedia Mater. Sci.* **7** (2014), p. 23-31.

[20] O. Dargaud, L. Cormier, N. Menguy, L. Galoisy, G. Calas, S. Papin, G. Querel, L. Olivi, "Structural role of Zr^{4+} as a nucleating agent in a $MgO–Al_2O_3–SiO_2$ glass-ceramics: A combined XAS and HRTEM approach", *J. Non-Cryst. Solids* **356** (2010), p. 2928-2934.

[21] P. Jollivet, L. Galoisy, G. Calas, F. Angeli, S. Gin, M. P. Ruffoni, N. Trcera, "Zirconium local environment in simplified nuclear glasses altered in basic, neutral or acidic conditions: Evidence of a double-layered gel", *J. Non-Cryst. Solids* **503–504** (2019), p. 268-278.

[22] L. Cormier, O. Dargaud, G. Calas, C. Jousseaume, S. Papin, N. Trcera, A. Cognigni, "Zr environment and nucleation role in aluminosilicate glasses", *Mater. Chem. Phys.* **152** (2015), p. 41-47.

[23] L. Cormier, B. Cochain, A. Dugué, O. Dargaud, "Transition elements and nucleation in glasses using X-ray absorption spectroscopy", *Int. J. Appl. Glass Sci.* **5** (2014), p. 126-135.

[24] S. Bhattacharyya, T. Hoche, J. R. Jinschek, I. Avramov, R. Wurth, M. Muller, C. Russel, "Direct evidence of Al-rich layers around nanosized $ZrTiO_4$ in glass: putting the role of nucleation agents in perspective", *Cryst. Growth Des.* **10** (2010), p. 379-385.

[25] O. Dargaud, L. Cormier, N. Menguy, G. Patriarche, G. Calas, "Mesoscopic scale description of nucleation processes in glasses", *Appl. Phys. Lett.* **99** (2011), article no. 021904.

[26] D. R. Neuville, L. Cormier, V. Montouillout, P. Florian, F. Millot, J.-C. Rifflet, D. Massiot, "Structure of Mg- and Mg/Ca aluminosilicate glasses: ^{27}Al NMR and Raman spectroscopy investigations", *Am. Mineral.* **93** (2008), p. 1721-1731.

[27] K. Liao, A. Masuno, A. Taguchi, H. Moriwake, H. Inoue, T. Mizoguchi, "Revealing spatial distribution of Al-coordinated species in a phase-separated aluminosilicate glass by STEM-EELS", *J. Phys. Chem. Lett.* **11** (2020), p. 9637-9642.

[28] L. Cormier, D. Ghaleb, J. M. Delaye, G. Calas, "Competition for charge compensation in borosilicate glasses: wide-angle X-ray scattering and molecular dynamics calculations", *Phys. Rev. B* **61** (2000), p. 14495-14999.

[29] M. Ficheux, E. Burov, G. Aquilanti, N. Trcera, V. Montouillout, L. Cormier, "Structural evolution of high zirconia aluminosilicate glasses", *J. Non-Cryst. Solids* **539** (2020), article no. 120050.

[30] A. Zandona, M. Moustrous, C. Genevois, E. Véron, A. Canizarès, M. Allix, "Glass-forming ability and ZrO_e saturation limits in the magnesium aluminosilicate system", *Ceram. Int.* **48** (2022), p. 8433-8439.

[31] Y. Yu, Z. Fang, C. Ma, H. Inoue, G. Yang, S. Zheng, D. Chen, Z. Yang, A. Masuno, J. Orava, S. Zhou, J. Qiu, "Mesoscale engineering of photonic glass for tunable luminescence", *NPG Asia Mater.* **8** (2016), article no. e318.

[32] K. D. Burgess, R. M. Stroud, M. D. Dyar, M. C. McCanta, "Submicrometer-scale spatial heterogeneity in silicate glasses using aberration-corrected scanning transmission electron microscopy", *Am. Mineral.* **101** (2016), p. 2677-2688.

[33] W. Jiao, P. Liu, H. Lin, W. Zhou, Z. Wang, T. Fujita, A. Hirata, H.-W. Li, M. Chen, "Tunable Nanoporous metallic glasses fabricated by selective phase dissolution and passivation for ultrafast hydrogen uptake", *Chem. Mater.* **29** (2017), p. 4478-4483.

[34] K. Liao, M. Haruta, A. Masuno, H. Inoue, H. Kurata, T. Mizoguchi, "Real-space mapping of oxygen coordination in phase-separated aluminosilicate glass: Implication for glass stability", *ACS Appl. Nano Mater.* **3** (2020), p. 5053-5060.

[35] T. I. Barry, J. M. Cox, R. Morrell, "Cordierite glass-ceramics - effect of TiO_2 and ZrO_2 content on phase sequence during heat treatment", *J. Mater. Sci.* **13** (1978), p. 594-610.

[36] V. V. Golubkov, O. S. Dymshits, A. A. Zhilin, T. I. Chuvaeva, A. V. Shashkin, "On the phase separation and crystallization of glasses in the $MgO–Al_2O_3–SiO_2–TiO_2$ system", *Glass Phys. Chem.* **29** (2003), p. 254-266.

[37] P. F. James, "Liquid-phase separation in glass-forming systems", *J. Mater. Sci.* **10** (1975), p. 1802-1825.

[38] G. H. Beall, B. R. Karstetter, H. L. Rittler, "Crystallization and chemical strenghtening of stuffed β-quartz glass-ceramics", *J. Am. Ceram. Soc.* **50** (1967), p. 182-190.

[39] V. G. Karpov, D. W. Oxtoby, "Nucleation in disordered systems", *Phys. Rev. B* **54** (1996), p. 9734-9745.

[40] I. Alekseeva, O. Dymshits, V. Golubkov, A. Shashkin, M. Tsenter, A. Zhilin, "Phase transformation in NiO and CoO doped magnesium aluminosilicate glasses nucleated by ZrO_2", *Glass Technol.* **46** (2005), p. 187-191.

[41] P. Li, I. W. Chen, J. E. Penner-Hahn, "X-ray-absorption studies of zirconia polymorphs. II. Effect of Y_2O_3 dopant on ZrO_2 structure", *Phys. Rev. B* **48** (1993), p. 10074-10081.

[42] T. Kawasaki, H. Tanaka, "Formation of a crystal nucleus from liquid", *Proc. Natl. Acad. Sci. USA* **107** (2010), p. 14036-14041.

[43] P. R. ten Wolde, D. Frenkel, "Enhancement of protein crystal nucleation by critical density fluctuations", *Science* **277** (1997), p. 1975-1978.

[44] L. Cormier, S. Zhou, "Transition metals as optically active dopants in glass-ceramics", *Appl. Phys. Lett.* **116** (2020), article no. 260503.

[45] C. Weigel, L. Cormier, G. Calas, L. Galoisy, D. T. Bowron, "Nature and distribution of iron sites in a sodium silicate glass investigated by neutron diffraction and EPSR simulation", *J. Non-Cryst. Solids* **354** (2008), p. 5378-5385.

[46] C. Weigel, L. Cormier, G. Calas, L. Galoisy, D. T. Bowron, "Intermediate-range order in the silicate network glasses $NaFe_xAl_{1-x}Si_2O_6$ ($x = 0, 0.5, 0.8, 1$): a neutron diffraction and empirical potential structure refinment modeling investigation", *Phys. Rev. B* **78** (2008), article no. 064202.

[47] M. Ahmadzadeh, A. Scrimshire, L. Mottram, M. C. Stennett, N. C. Hyatt, P. A. Bingham, J. S. McCloy, "Structure of $NaFeSiO_4$, $NaFeSi_2O_6$, and $NaFeSi_3O_8$ glasses and glass-ceramics", *Am. Mineral.* **105** (2020), p. 1375-1384.

[48] Z. Yang, B. Wang, A. N. Cormack, "The local structure of Fe in Li(Al, Fe)Si_2O_6 glasses from molecular dynamics simulations", *J. Non-Cryst. Solids* **444** (2016), p. 16-22.

[49] P. A. Bingham, J. M. Parker, T. Searle, J. M. Williams, K. Fyles, "Redox and clustering of iron in silicate glasses", *J. Non-Cryst. Solids* **253** (1999), p. 203-209.

[50] A. Montenero, M. Friggeri, D. C. Giori, N. Belkhiria, L. D. Pye, "Iron-soda-silica glasses: Preparation, properties, structure", *J. Non-Cryst. Solids* **84** (1986), p. 45-60.

[51] G. Calas, "Electron paramagnetic resonance", *Rev. Mineral.* **18** (1988), p. 513-572.

[52] K. Sakaguchi, T. Uchino, "Compositional dependence of infrared absorption of iron-doped silicate glasses", *J. Non-Cryst. Solids* **353** (2007), p. 4753-4761.

[53] V. Vercamer, G. Lelong, H. Hijiya, Y. Kondo, L. Galoisy, G. Calas, "Diluted Fe^{3+} in silicate glasses: structural effects of Fe-redox state and matrix composition. An optical absorption and X-band/Q-band EPR study", *J. Non-Cryst. Solids* **428** (2015), p. 138-145.

[54] M. Wilke, F. Farges, P.-E. Petit, G. E. Brown, F. Martin, "Oxidation state and coordination of Fe in minerals: An Fe K-XANES spectroscopic study", *Am. Mineral.* **86** (2001), p. 714-730.

[55] V. Vercamer, "Spectroscopic and structural properties of iron in silicate glasses", PhD Thesis, Université Pierre et Marie Curie - Paris VI, 2016, https://tel.archives-ouvertes.fr/tel-01458771.

[56] G. Vankó, F. M. F. de Groot, S. Huotari, R. J. Cava, T. Lorenz, M. Reuther, "Intersite 4p-3d hybridization in cobalt oxides: a resonant X-ray emission spectroscopy study", 2008, preprint, https://arxiv.org/abs/0802.2744.

[57] R. G. Burns, *Mineralogical Applications of Crystal Field Theory*, 2nd ed., Cambridge University Press, Cambridge, 1993.

[58] W. Loewenstein, "The distribution of aluminum in the tetrahedra of silicates and aluminates", *Am. Mineral.* **39** (1954), p. 92-96.

[59] R. McMillan, M. Amini, D. Weis, "Splitting obsidian: assessing a multiproxy approach for sourcing obsidian artifacts in British Columbia", *J. Archaeol. Sci. Rep.* **28** (2019), article no. 102040.

[60] M. Duttine, G. Villeneuve, G. Poupeau, A. M. Rossi, R. B. Scorzelli, "Electron spin resonance of Fe^{3+} ion in obsidians from Mediterranean islands. Application to provenance studies", *J. Non-Cryst. Solids* **323** (2003), p. 193-199.

[61] J. R. Regnard, F. Chavez-Rivas, J. Chappert, "Study of the oxidation states and magnetic properties of iron in volcanic glasses: Lipari and Teotohuacan obsidians", *Bull. Minéral.* **104** (1981), p. 204-210.

[62] D. Di Genova, A. Caracciolo, S. Kolzenburg, "Measuring the degree of "nanotilization" of volcanic glasses: understanding syn-eruptive processes recorded in melt inclusions", *Lithos* **318–319** (2018), p. 209-218.

[63] A. Ferk, R. Leonhardt, K.-U. Hess, D. B. Dingwell, "Paleointensities on 8 ka obsidian from Mayor Island, New Zealand", *Solid Earth* **2** (2011), p. 259-270.

[64] F. Caceres, F. B. Wadsworth, B. Scheu, M. Colombier, C. Madonna, C. Cimarelli, K.-U. Hess, M. Kaliwoda, B. Ruthensteiner, D. B. Dingwell, "Can nanolites enhance eruption explosivity?", *Geology* **48** (2020), p. 997-1001.

[65] L. Galoisy, G. Calas, "The unique speciation of iron in calc-alkaline obsidians", *Chem. Geol.* **559** (2021), article no. 119925.

[66] B. Wang, S. Qu, "Discrete dipole approximation simulations of absorption spectra and local electric field distributions of superparamagnetic magnetite nanoparticles", *Laser Phys.* **23** (2013), article no. 045901.

[67] G. Amthauer, G. R. Rossman, "Mixed valence of iron in minerals with cation clusters", *Phys. Chem. Miner.* **11** (1984), p. 37-51.

[68] S. M. Mattson, G. R. Rossman, "Identifying characteristics of charge transfer transitions in minerals", *Phys. Chem. Miner.* **14** (1987), p. 94-99.

[69] P. A. Cox, "Electron transfer between exchange-coupled ions in a mixed-valency compound", *Chem. Phys. Lett.* **69** (1980), p. 340-343.

[70] X. Lu, L. Deng, J. Du, "Effect of ZrO_2 on the structure and properties of soda-lime silicate glasses from molecular dynamics simulations", *J. Non-Cryst. Solids* **491** (2018), p. 141-150.

[71] P. H. Gaskell, "Structure, glass formation and properties", *J. Non-Cryst. Solids* **192–193** (1995), p. 9-22.

[72] G. S. Henderson, G. Calas, J. F. Stebbins, "The structure of silicate glasses and melts", *Elements* **2** (2006), p. 269-273.

[73] B. E. Warren, J. Biscoe, "Fourier analysis of X-ray patterns of soda-silica glass", *J. Am. Ceram. Soc.* **21** (1938), p. 259-265.

[74] A. F. Wells, *Structural Inorganic Chemistry*, 4th ed., Clarendon Press, Oxford, 1975.